

Numerical Methods of Visco-elastic Segments on Water Hammer Pressures

Jalal Rahimi Firuz*, Saeed reza Sabagh Yazdi**, Alireza Keramat***

ARTICLE INFO

Article history:

Received:

April 2020.

Revised:

May 2020.

Accepted:

June 2020.

Keywords:

Transient flow

Water hammer

Visco-elastic pipe

MOC

Pressure

Abstract:

Water hammer is a phenomenon accompanied by damage, vibration and noise. In order to deal with this phenomenon, different solutions have been proposed. Mechanical behavior of pipe material can significantly affect pressure responses of the pipe system during the transient flow. Utilizing viscoelastic pipe segments for attenuating the water hammer pressure may be considered as a damping mechanism alternate. The aim of this study is investigating the use of viscoelastic materials such as polyethylene in absorption of water hammer energy. The governing equations in this phenomenon are comprised of Continuity Equation and Momentum Equation. Discretization of the equations is done/performed by employing the Method of Characteristics (MOC). Verification of the developed numerical method is done/executed by comparing the results with the empirical results obtained from another study preformed earlier. The comparison between the results demonstrates that the numerically obtained results have acceptable accuracy. Also the effect of variations in the values of different parameters on decreasing the induced pressure is investigated. Numerous studies have been conducted on visco-elatic pipes; the innovation in this study however, is combining the use of visco-elastic and elastic material in the same pipe for cushioning the effects of water hammer.

1. Introduction

“Water hammer,” is a pressure surge created along the pipe when the valve is suddenly closed or while pumping systems are run resulting in an increase or decrease in pressure periodically. The word is derived from a French word and it is among the most widespread causes of damages to pipelines. Surge tanks (fig.1) and flywheels are common but costly solutions to encounter the forgoing phenomenon. This paper proposes a new approach to not only alleviate the negative impacts of the phenomenon but also revise or eliminate common equipment by virtue of using polymeric pipes. Changes in the content of viscoelastic pipes occur due to increase in pressure, which results in damping to restore pressure

We believe/infer that we may have found an effective solution to counter the water hammer phenomenon using the striking feature of poly-ethylene pipes namely, viscosity.



Fig. 1: Construction steps of a surge tank

It should be noted that the foregoing solution is only applicable for over ground pipes. Underground poly ethylene pipes work like an elastic pipe, so, in order to achieve desired results from the proposed approach, it is

* Corresponding Author: M.Sc., Faculty of Civil Engineering, K. N. Toosi University of Technology, Tehran, Iran, Email: rahimifiroz@gmail.com

** Professor, Faculty of Civil Engineering, K. N. Toosi University of Technology, Tehran, Iran.

*** Assistant Professor, Faculty of Civil Engineering, Jundishapur University of Technology, Dezful, Iran.

necessary to use viscoelastic pipes. However, pipelines, especially water pipes used to transfer water to plants, are for the most part underground pipes, hence viscoelastic pipes need to be used in a small part of the pipeline. A new effective method to deal with water hammer phenomenon is using lengths of polyethylene pipe along the pipeline. As a result, the compressive wave energy generated by the water hammer phenomenon along the foregoing pipes is dissipated by the deformation of viscoelastic portion of the pipeline.

Consequently, there is no need to install pressure reduction equipment, mainly due to a decline in pressure changes throughout the pipe and a decrease in positive and negative maximum amplitude. It must be noted that such time-dependent behaviors of viscoelastic material rely mostly on its especial molecular structure. The foregoing striking feature of these materials is completely different from other environmental phenomena, like fatigue and corrosion, causing deformation [1]. The present research aims to investigate the effects of using a piece of viscoelastic pipe along the pipeline to alleviate amplitude of positive and negative pressures caused by immediate closure of valves situated at the end of the pipeline, assisted with mathematical modeling and Method of Characteristics (MOC). In a research Covas [2] proposed the Method of Characteristics (MOC) to depict modeling of viscoelastic pipes' wall behavior for unsteady flows.

The present research takes a new look at the water hammer phenomenon occurring in the viscoelastic pipes; therefore the impact of environmental pipe wall strains was modeled by Kelvin–Voigt elements. The model stimulates the viscoelastic behavior by virtue of a set of springs and dampers. The two equations of continuity and momentum conservation are used in this paper, thus like a source term, the impact of viscoelastic behavior enters into the conservation of mass equation.

According to the modeling method, creep functions of a viscoelastic pipe are calibrated by conducting an unsteady flow test. The forgoing method was later revised by Soares [3]. In a comprehensive research Keramat [4] assessed numerical and experimental impacts concerning separation of the liquid column of viscoelastic pipes. The MOC modeling method was exercised to check impacts of damping features of viscoelastic pipes on decline in compression changes caused by immediate closure of the valve at the end of the pipe.

The aim of the paper is to first examine equations concerning unsteady flows in the elastic and viscoelastic pipes as well as to describe the changes in the viscoelastic behavior of poly-ethylene pipes by the time and then to study numerical analysis of equations using the MOC method [5,6].

The water hammer phenomenon and the impacts thereof on the changes in pressure as a function of time in such parts of the pipeline containing viscoelastic pipes varying in length

were completely studied by the virtue of revised numerical tests. The present research aims to depict pressure fluctuations in the pipeline by using three different combinations of elastic and viscoelastic pipes [7, 8].

2. Equations concerning unsteady flows

2.1. Equations concerning unsteady flows of the elastic pipes

The Mathematical model assumptions in elastic and viscoelastic tubes are as below:

- The proposed model, in the present research, is valid for the circular cross section pipes.
- There is no lateral flow, apart from a one dimensional flow along the pipe axis
- Distribution of velocity is the same at the cross section.
- The valve and pipe are both restrained at the axial position.
- It is assumed that both room and fluid temperatures are steady within the simulation period.
- There is only one coordinate system along the pipe axis for this one-dimensional model as to qualify its differential relations.
- Effects of structural interference deformations such as flexural strength, rotary inertia as well as axial and shear deformations, are ignored.

Equations concerning unsteady flows of the elastic pipes are obtained by solving the two mass and the momentum conservation equations [9].

$$\frac{\partial H}{\partial x} + \frac{1}{gA} \frac{\partial Q}{\partial t} + \frac{fQ|Q|}{2DA^2g} = 0 \quad (1)$$

$$\frac{1}{A} \frac{\partial Q}{\partial x} + \frac{g}{C^2} \frac{\partial H}{\partial t} = 0 \quad (2)$$

$$C = \sqrt{\frac{\frac{K}{\rho}}{1 + \left(\frac{kD}{Ee}\right)}} \quad (3)$$

Where:

Q is volumetric flow (m³/s), A is the cross-section of pipe (m²), g is gravity (m/s²), D is pipe diameter (m), H is tank height (m), C is sound velocity (m/s), t is time (s), x is pipe length (m), f is the Darcy's Weisbach coefficient, e is pipe thickness, K is fluid's volumetric module and E is fluid's elasticity module (Pa).

2.2. Equations concerning viscoelastic pipes

The theory about how pipe wall shows a viscoelastic behavior against the unsteady flow depends upon the following hypotheses:

- To obtain the differential equations, a linear-viscoelastic thin-wall pipe is hypothesized.
- All differential equations are linear, apart from $\left(\frac{fQ|Q|}{2DA^2g}\right)$ indicating a decline, mainly because of friction between the fluid and pipe wall. It should also be noted that the existence of non-boundary conditions, i.e., closure of the valve, will lead to a non-linear problem.

In providing a valid service using a viscoelastic wall assembly (eg polyethylene), unsteady flow equations should direct the use of assumptions, re-select different options and also be able to apply them [10].

The equilibrium flow equations in the viscoelastic tube, like the elastic tube, consist of mass and mass size stability equations and are presented as follows [11, 12]:

$$\frac{1}{A} \frac{\partial Q}{\partial z} + \frac{\rho g}{K} \frac{\partial H}{\partial t} + 2 \frac{\partial \varepsilon_\theta}{\partial t} = 0 \quad (4)$$

$$g \frac{\partial H}{\partial z} = -2 \frac{fQ|Q|}{2DA^2} + \frac{1}{A} \frac{\partial Q}{\partial t} \quad (5)$$

The last term of equation 4, $\left(\frac{\partial \varepsilon_\theta}{\partial t}\right)$, describes a rate of environmental strain change demonstrating elastic and slow behavior. Environmental strain in the elastic pipes works as an index of the fluid pressure. However, a delay occurs in the viscoelastic pipes as a function changes in the fluid pressure [13].

The link between tension and strain of linear viscoelastic materials consists of high degree time differences thereof. As it can be seen in Eq.6, an alternative form is obtained from the link between tension and strain using Laplace reduction and its reverse [14].

$$\varepsilon(t) = \sigma(t)J(0) + \int_0^t \sigma(t-s) \frac{dJ(s)}{ds} ds = (\sigma * dJ)(t) \quad (6)$$

$$= (J * d\sigma)(t)$$

Where, “*” and “d” indicate convolution and stiles-convolution operators, respectively, which are studied later. Unlike a common convolution, a stiles-convolution operator has an additional term, $\sigma(t)J(0)$, i, indicating system immediate reaction, , that is, elastic. The equation 6 can be written as follows by entering a correspondence creep equation, $J(t)$, according to a generalized Kelvin-Voigt model [15].

$$J(t) = J_0 + \sum_{k=1}^{N_{kv}} J_k \left(1 - e^{-\frac{t}{\tau_k}}\right) \quad (7)$$

Where, $J_0 = 1/E$, $J_k = 1/E_k$, E_k , t , τ_k , indicates immediate response of viscoelastic material, $J_k = 1/E_k$ is comparative creep of the spring as to Kth element of Kelvin-Voigt equation, E_k is the elasticity module of Kth spring, t is time, delay and τ_k is time of Kth damper, which is defined as $\tau_k = \frac{\mu_k}{E_k}$.

Regarding hypotheses about thick-wall pipes and the link between environmental tensions in an impacted pipe, hoop strain in a thick-wall pipe is computed as follows (3, 4):

$$\varepsilon_\varphi = (1 - \vartheta^2) \left(\frac{\rho g D}{2e} \tilde{H} * dJ\right), \tilde{H} = H - H_0 \quad (8)$$

Where, H, H0 indicate head pressure, initial head pressure and Poisson relation. Thus, substituting (8) into (4), we obtain the mass conservation equation:

Where,

$$\frac{1}{A} \frac{\partial Q}{\partial z} + \frac{\rho g}{K} \frac{\partial H}{\partial t} + (1 - \vartheta^2) \frac{\rho g D}{e} \frac{\partial}{\partial t} (\tilde{H} * dJ) = 0 \quad (9)$$

It can be written as equation 10, where stiles-convolution is applied:

$$\frac{1}{A} \frac{\partial Q}{\partial z} + \frac{g}{C^2} \frac{\partial H}{\partial t} = -(1 - \vartheta^2) \frac{\rho g D}{e} \frac{\partial I_{\tilde{H}}}{\partial t} \quad (10)$$

Where, C indicates velocity of wave distribution in a viscoelastic pipe and $I_{\tilde{H}}$ is computed as follow:

$$C = \sqrt{\frac{\frac{k}{\rho}}{1 + \left(\frac{kD}{Ee}\right)}} \quad (11)$$

$$I_{\tilde{H}}(t) = \int_0^t \tilde{H}(t-s) \frac{dJ(s)}{ds} ds$$

$$= \sum_{k=1}^{N_{kv}} \left(\frac{J_k}{\tau_k} \int_0^t \tilde{H}(t-s) e^{-\frac{s}{\tau_k}} ds \right) \quad (12)$$

$$= \sum_{k=1}^{N_{kv}} I_{\tilde{H}k}(t)$$

Insertion of J into (7) yields the third term of (12). Accordingly, both conservation equations of momentum (4) and corrected mass (10) could be solved to compute the two Q and H unknowns [16, 17].

3. Numerical solution of unsteady flow by means of MOC

3.1. Numerical solution of unsteady flow in the elastic pipes by means of MOC:

By virtue of the MOC method (1, 3) both Q and H unknown parameters are obtained for each spatial and temporal steps (point (p)).

$$Q_P = \frac{1}{2} \left[(V_L + V_R) + \frac{Ag}{C} (H_L - H_R) - \frac{f\Delta t}{2DA} (Q_R | Q_R| + Q_L | Q_L|) \right] \quad (13)$$

$$H_P = \frac{1}{2} \left[(H_L + H_R) + \frac{g}{AC} (Q_L - Q_R) - \frac{Cf\Delta t}{2DA^2g} (Q_L|Q_L| - Q_R|Q_R|) \right] \quad (14)$$

R and L demonstrate left and right nodes of the node (p), respectively (fig.2). Stability condition for the explicit solution by means of MOC is:

$$C \frac{\Delta t}{\Delta x} \leq 1 \quad (15)$$

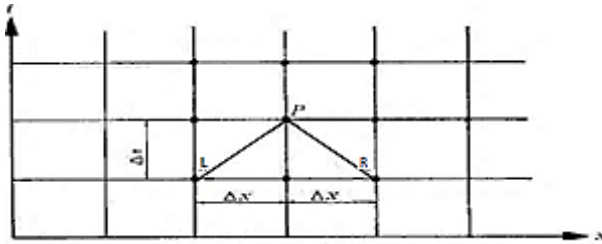


Fig. 2: position of the characteristic lines than network nodes

3.2. Numerical solution of unsteady flow of viscoelastic pipes using MOC:

In order to run a temporal analysis, convolution integral in equation 12 needs to be written as a direct term of unknown parameters, otherwise there will be a series of integral equations which would be difficult to solve. Thus, the simplest way is to write them in the form of terms containing unknown parameters in the current calculations and calculated amounts in the past. With regard to the unknown parameters in the present, the term containing convolution integral in equation 12 is computed by the virtue of the following relation [18]:

$$\begin{aligned} \frac{\partial I_{\tilde{H}}(t)}{\partial t} \approx \tilde{H}(t) \left(\frac{J_k}{\Delta t} \left(1 - e^{-\frac{\Delta t}{\tau_k}} \right) \right) \\ + \tilde{H}(t - \Delta t) \left(\frac{J_k}{\tau_k} e^{-\frac{\Delta t}{\tau_k}} \right) \\ - \frac{J_k}{\Delta t} \left(1 - e^{-\frac{\Delta t}{\tau_k}} \right) - \frac{e^{-\frac{\Delta t}{\tau_k}}}{\tau_k} I_{Hk}(t - \Delta t) \end{aligned} \quad (16)$$

Thus, the MOC method is used to solve these equations. It must be noted that, although the MOC method for the viscoelastic pipes is exercised in much the same as elastic ones, in this case derivative of the term containing convolution integral is written as equation (16) regarding pressure head for an unknown t. Corresponding to the MOC method, first, the two differential equations are reduced into two separate but partial differential equations (an univariate equation), and then written as a finite difference form on the two C+ , C- characteristic lines [19].

$$C^+: Q_P = -C_{a+} H_P + C_P \quad (17)$$

$$C^-: Q_P = C_{a-} H_P + C_n \quad (18)$$

Where, $Q = AV$ demonstrates the fluid flow rate, P index implies the unknown parameters and C_P, C_n, C_{a-}, C_{a+} are obtained by means of previous computed amounts as follow [4]:

$$C_P = \frac{Q_L + BH_L + C'_{P1} + C''_{P1} + C'''_{P1}}{1 + C'_{P2} + C''_{P2}} \quad (19)$$

$$C_n = \frac{Q_R + BH_{A2} + C'_{n1} + C''_{n1} + C'''_{n1}}{1 + C'_{n2} + C''_{n2}} \quad (20)$$

$$C_{a+} = \frac{B + C''_{P2}}{1 + C'_{P2} + C''_{P2}} \quad (21)$$

$$C_{a-} = \frac{B + C''_{n2}}{1 + C'_{n2} + C''_{n2}} \quad (22)$$

$$B = \frac{gA_f}{C} \quad (23)$$

Where, p and n indices demonstrate negative and positive characteristic lines. Unknowns containing L and R indices are corresponding previous calculated points on lines C+(C-). In addition to this, ' ' , ' ' ' demonstrate terms as to a quasi-steady friction model (Darcy's Weissbach equation), unsteady friction (not mentioned in this paper) and mechanical behavior of pipe wall, respectively. The following represents relations for computing each data used in the forgoing relations [4].

$$C'''_{P2} = \frac{D}{e} A \rho g (1 - \theta^2) C \Delta t a_1 \quad (24)$$

$$C'_{P2} = R |Q_{A1}| \Delta t \quad (25)$$

$$C'''_{P1} = \frac{D}{e} A \rho g (1 - \theta^2) C \Delta t a_2 \quad (26)$$

$$C'''_{P2} = C'''_{n2} \quad (27)$$

$$C'''_{n1} = -C'''_{P1} \quad (28)$$

$$C_{n2} = R |Q_{uA2}| \Delta t \quad (29)$$

Where, a_1 and a_2 represent characteristics of viscoelastic pipes and are determined according to data obtained from the previous time step [20].

$$a_1 = \sum_{k=1}^{N_{KV}} \frac{J_k}{\Delta t} \left(1 - e^{-\frac{\Delta t}{\tau_k}} \right) \quad (30)$$

$$\begin{aligned} a_2 = -H_0 \sum_{k=1}^{N_{KV}} \frac{J_k}{\tau_k} e^{-\frac{\Delta t}{\tau_k}} + H(t) \sum_{k=1}^{N_{KV}} \left(\frac{J_k}{\tau_k} e^{-\frac{\Delta t}{\tau_k}} - \frac{J_k}{\Delta t} \left(1 - e^{-\frac{\Delta t}{\tau_k}} \right) \right) \\ - \sum_{k=1}^{N_{KV}} \frac{e^{-\frac{\Delta t}{\tau_k}}}{\tau_k} I_{Hk}(t - \Delta t) \end{aligned} \quad (31)$$

$$\begin{aligned}
I_{\text{HK}}(t - \Delta t) \approx & (H(t - \Delta t) - H_0) \left(J_k \right. \\
& \left. - \tau_k \frac{J_k}{\Delta t} \left(1 - e^{-\frac{\Delta t}{\tau_k}} \right) \right) \\
& + (H(t - 2\Delta t) - H_0) \left(-J_k e^{-\frac{\Delta t}{\tau_k}} \right. \\
& \left. + \tau_k \frac{J_k}{\Delta t} \left(1 - e^{-\frac{\Delta t}{\tau_k}} \right) \right) \\
& + e^{-\frac{\Delta t}{\tau_k}} I_{\text{HK}}(t - 2\Delta t)
\end{aligned} \quad (32)$$

4. Validation of modeling results

To assess validation of modeling result, there is a need to compare results of computed pressure with experimental measurements reported by researchers, then if test results are assumed to be true, numerical model error is estimated by the virtue of $\frac{H_L - H_p}{H_L} * 100$, where H_L and H_p are head pressure of the experimental and numerical models, respectively [21].

Therefore, unsteady pressure numeric modeling results concerning an elastic pipe were first compared to Adam Koviski's experimental model, and then, unsteady pressure numeric modeling results of a viscoelastic pipe were weighed with Ms. Covas's experimental model.

4.1. Unsteady flow in an elastic pipe

Adam Koviski's experimental measurement results were used to validate an unsteady flow in an elastic pipe made of copper [1]. The Darcy- Weisbach quasi-steady friction model applies to compute friction terms in the present modeling. The forgoing experiment properties are highlighted in Table 1 [9]

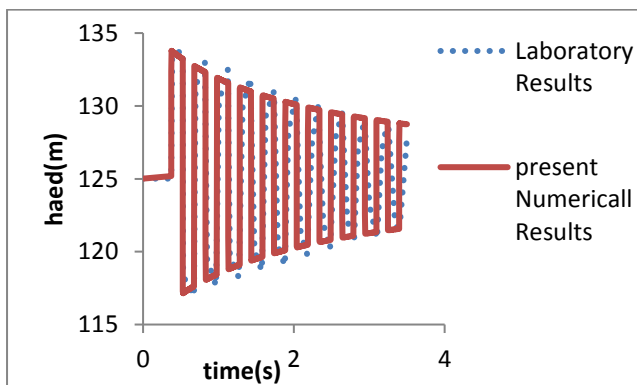


Fig. 3: Comparison between an elastic pipe line experimental diagrams at the valve point with Darcy- Weisbach quasi-steady friction model

Table 1: Input data concerning the experiment for studying water hammer phenomenon in an elastic pipe.

Friction coefficient	0.03
Tank head	127.42 m

Pipe wall thickness	1mm
Valve closure time	0.003 s
Flow rate of a steady flow	1.31s
Pipe inside diameter	16mm
Poisson ratio	0.46
Yang module	120GPa
Pipe length	98.11 m

The highest level of numerical modeling error is 0.643. The error average between the two diagrams of fig.3 is nearly 0.326 [5].

4.2. An unsteady flow in a viscoelastic pipe

To validate an unsteady flow in a viscoelastic pipe, measurement results of an experimental model conducted by Mrs. covas [10] at the laboratory of London Imperial College were used. The model was a simple tank-pipe-valve system consisting of a poly-ethylene pipe line. Also Table 2 inputs data concerning the Imperial College experiment in order to study the water hammer phenomenon in a viscoelastic pipe (the entire length of the pipe is 271.5 m).

Table 2: Maximum pressure head at the end of elastic, viscoelastic and 80/20% elastic-viscoelastic pipes

Friction coefficient	0.02	Tank head	45m
Valve closure time	0.09s	Flow rate of a steady flow	10.1 l.s-1
Poisson ratio	0.46	Yang module	1.43 GPa
Pipe wall thickness	6.3	Pipe inside diameter	50.6 mm

There are two main methods to measure τ_k (s) and J_k (comparative creep coefficient). The first is known as water hammer experiment [7]. In the foregoing experiment, an unsteady flow is generated in the system when the studied pipe in the hydraulic laboratory is closed immediately. Then, pressure fluctuations are dealt with using a numerical model and introducing a reverse problem into calibration of creep coefficient based on computing and observational data.

Table 3: Values of comparative creep and delay time

τ_k (s)	$\tau_1=0.05$ s	$\tau_2=0.5$ s	$\tau_3=1.5$ s	$\tau_4=5$ s	$\tau_5=10$ s
J_k (10 ⁻¹⁰ Pa-1)	$J_1=1.057$	$J_2=1.054$	$J_3=0.905$	$J_4=0.262$	$J_5=0.746$

So, it should be said that unknown parameters, that is to say, comparative creep coefficients, are obtained when a value of pressure and flow rate per time are available. A more comprehensive assessment is made by conducting the water hammer experiment for a special pipe, mainly because the viscoelastic behavior crucially depends on the variables such as temperature, support condition, initial flow rate and lack of uniformity in pipe's materials [4, 7]. In the experiment done/performed at London Imperial College, researchers succeeded in defining comparative creep functions of the

studied pipe by means of water hammer experiments. The next method is the creep mechanical experiment, which is generally done at the pipe manufacturing plant [22]. Creep strain coefficients for the foregoing test with five Kelvin-Voigt elements at 20 seconds intervals are outlined in Table 3.

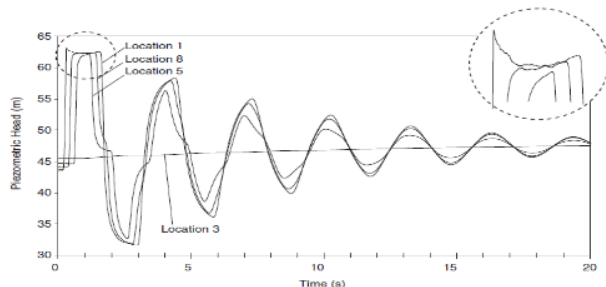


Fig. 4: experimental measurements of pressure changes at various locations for a viscoelastic pipe; (location 1: valve, location 3: tank, location 5: at the distance of 16 m from the tank, location 8: at a distance of 196 m from the tank)

As shown in fig.4, 4 four diagrams measured in the laboratory by Ms. Covas for four different locations are available for a viscoelastic pipe (location 1: at the end of pipe line, location 3: tank, location 5: at the distance of 16 m from the tank, location 8: at the distance of 196 m from the tank).

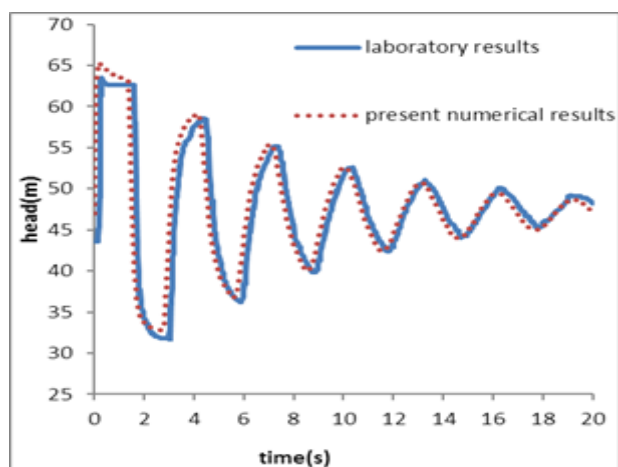


Fig. 5: Comparing reported pressure results using the numerical model at the end of the viscoelastic pipe line (valve) with the experimental measurements [10].

According to Fig.5, it can be seen that the pressure of the valve was first measured by the foregoing numerical model (krant 1) and then compared with the reported experimental values by Mrs. Covas [3]. Results are not in complete agreement with numerical model of Mrs. Covas [7], mainly because of some numerical discrepancies. As shown in Fig. 5, errors of the proposed model are either minor or significant at different points. The highest level of difference between the two diagrams is 0.21%. As the results of the present model and experimental data (Fig.4) were collected at two different times, average error of Fig. 5 is

approximately 0.16%. Generally, behavior and trend of the two diagrams are the same.

5. Model sensitivity to effective parameters

In order to examine the sensitivity of the expanded model, a pipe line located at the downstream of a tank containing both elastic and viscoelastic pipes and a terminative valve is used. This is done in two steps. The first is to compare the pressure diagram of a system consisting of 20% and 80% viscoelastic and elastic pipes, respectively, with two separate viscoelastic and elastic systems. The impact of using a different length of viscoelastic pipe in the combinational system is studied in the next step. For the studied numerical model, elastic and viscoelastic pipes are made of high density steel and poly-ethylene, (SDR11, PE100 NP16, respectively).

5.1. First step

The test is first carried out for all three different combinations of elastic and viscoelastic pipes, and then numerical results are compared as a pressure/time diagram. It should be noted that SDR is the ratio of the pipe outside diameter as a function of its thickness. The figure below represents test results for elastic and viscoelastic pipes and a 20% viscoelastic pipe.

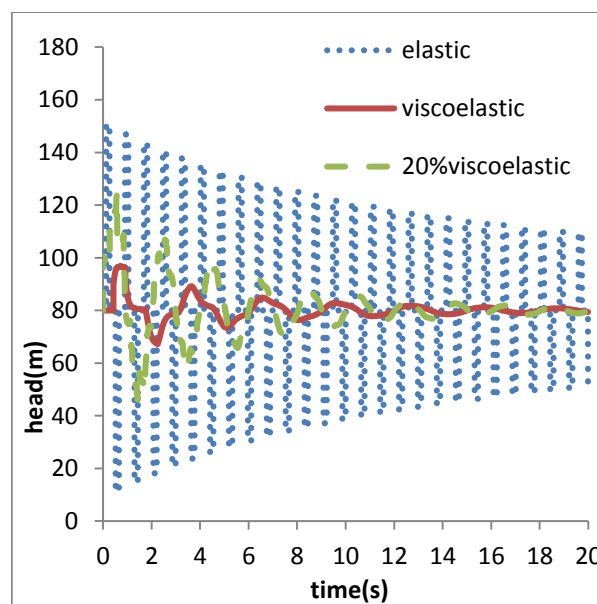


Fig. 6: Reported pressure changes at the terminal valve for all three elastic, viscoelastic and a 80/20 combination of elastic-viscoelastic pipe

As shown in Fig.6, considering a completely elastic pipe line, the valve pressure is slowly damped and the maximum amount of pressure is raised up to 151.41 m. By observing

the diagram of test, where only 20% of the end part of the pipe line is viscoelastic, the maximum pressure is reached at 124.15 m; thus, it can be seen that a 33.71 m decline was observed in the highest pressure level compared to a whole elastic pipe line.

When only 20% of the end part thereof is made of viscoelastic pipe, a $\frac{H_e - H_v}{H_e} * 100 = 22.26\%$ decline is observed in pressure, so its damping is more than a whole elastic pipeline. It should also be noted that, terms H_e and H_v in the foregoing equation suggest pressure head of an elastic and viscoelastic pipe line, respectively. As follows from the figures shown above, there was a steep decline in the pressure amplitude at the valve location, and the maximum amount of Pressure was 100.47. Table 2 suggests changes in the maximum amount of pressure head for the three studied cases.

Table 5: Maximum amount of pressure head at the valve location to examine sensitivity of viscoelastic part of the pipe line

Diagram	Head maximum	Ratio of increased pressure to a 100% viscoelastic pipe
Elastic pipe	151.41	51
80/20 ratio of elastic-viscoelastic pipe	124.51	24
Viscoelastic pipe	100.47	-

5.2. Second step

As shown/displayed in Fig. 7, to conduct a second sensitivity test, modeling results are presented as a pressure diagram at the valve location for three following modes: 80/20% elastic-viscoelastic; 90/10% elastic-viscoelastic; 95/5% elastic-viscoelastic. The graphs suggest that there is a link between length of the viscoelastic pipe and pressure. As can be seen, an increase in the length of the viscoelastic part of the pipe line will result in decreased pressure and increased damping rate. Table 2 summarizes the maximum pressure for each diagram of Fig.7.

Table 6: Maximum amount of pressure head at the valve location to examine sensitivity of viscoelastic part of the pipe line

Diagram	Maximum pressure (m)
80 %elastic + 20% viscoelastic pipe	124.51
90 %elastic + 10% viscoelastic pipe	135.78
95 %elastic + 5% viscoelastic pipe	144.13

The data shown in Table 5 suggests that there is a link between length of the viscoelastic part of the pipe line and decrease in the maximum pressures, which implies the profound impact of the viscoelastic pipes on decrease in the maximum amount of pressure.

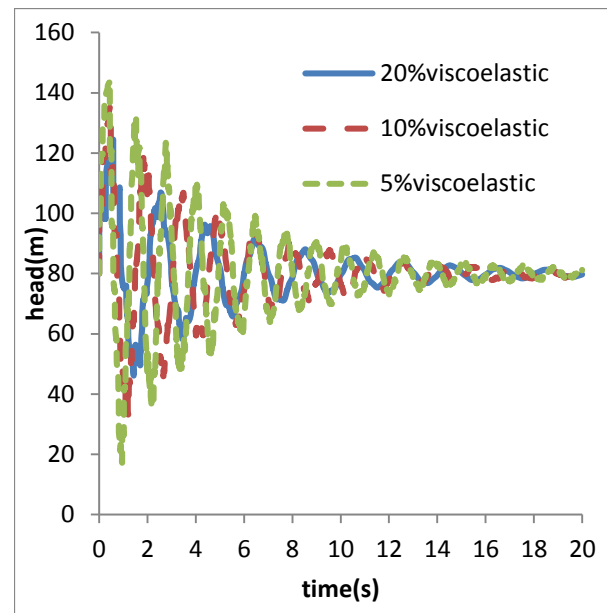


Fig. 7: Pressure changes at the valve location to study the results sensitivity to the viscoelastic length of the pipe

6. Comparing maximum and minimum pressures at different parts of the pipe

It is reasonable to expect that as the distance of the water hammer occurrence point increases from valve location, a further decrease is observed in maximum and minimum amounts of pressure, and pressure fluctuation tends to shift onto the tank pressure thereof. For this, changes in the maximum and minimum pressures as a function of time are plotted for a system consisting of a viscoelastic pipe, tank and valve. Thus, four points of the pipe are studied: at a distance of 271.5 m from the tank (valve), at a distance of 150 m from the tank and at a distance of 20 m from the tank and the tank itself.

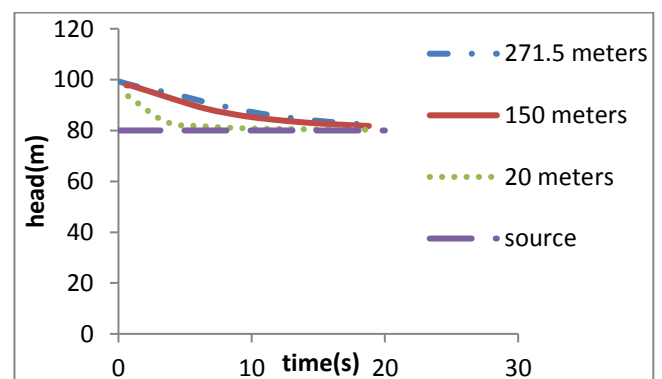


Fig. 8: changes in the maximum pressure to the time

6.1. Changes in maximum pressure to time

As can be seen from Fig. 8 and 9, maximum and minimum pressures are further decreased and pressure arising from

water hammer phenomenon considerably fluctuates around initial pressure (tank pressure) when the studied point is closer to the tank. Fig. 8 suggests that, as the distance from the studied point is decreased, so does the required time for the occurrence of maximum pressure, when it is increased; thus it is evident that there is a significant link between the studied location and required time to observe maximum pressure.

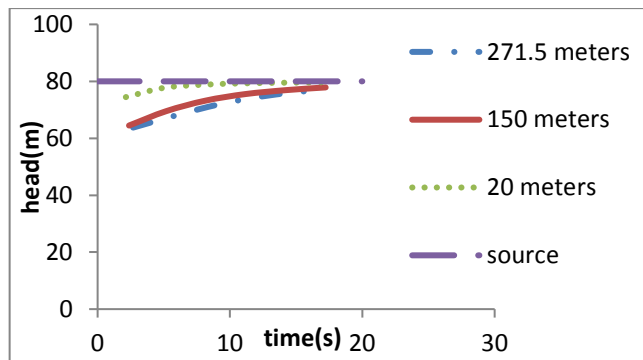


Fig. 9: Changes in the minimum pressure to the time

7. Conclusion

A series of loading and unloading cyclic waves are created in the system when the water hammer phenomenon occurs in the pipe line. The structural reaction of the pipe wall to load fluctuations plays a pivotal role in the formation and depreciation of compressive signals arising from the water hammer. The present research addressed the impacts of a pipe line consisting of elastic and viscoelastic pipes on pressure fluctuations arising from the water hammer phenomenon.

Moreover, equations concerning unsteady flow along elastic and viscoelastic pipes were studied. They were rewritten considering the conditions of viscoelastic pipes by the virtue of Kelvin-Voigt expanded mechanical model. A MOC method was also used to expand a numerical model to solve equations. Model results were assessed by comparing experimental measurements conducted at London Imperial College for a flow in a whole viscoelastic pipe.

The impact of the viscoelastic behavior on the tail end of the pipe line on balancing maximum and minimum pressures for different lengths of a viscoelastic pipe was studied by the virtue of introducing a problem containing tank, elastic pipe, viscoelastic pipe and end valve.

Numerical model results represent that using a viscoelastic pipe adjacent to the tail end of the pipe line (near the valve) has a profound effect on a decrease in the maximum and minimum pressures. The findings are most important in terms of designing pipelines such that there will be a considerable decrease in constructing expensive surge tanks and cost thereof. More experiments will be required with

regards to using proper length of viscoelastic pipes for the pipelines of power plants and pumping stations.

References:

- [1] Bergant, A., Tijsseling, A., Vítkovský, J., Covas, D., Simpson, A., Lambert, M. "Further investigation of parameters affecting water hammer wave attenuation, shape and timing" *IAHR journal of hydraulic research* 46, 2008, vol. 3, pages 382–391.
- [2] Covas, D., Stoianov, I., Mano, J., Ramos, H., Graham, N., Maksimovic. "The dynamic effect of pipe-wall viscoelasticity on hydraulic transients Part I—Experimental analysis and creep characterization "proceedings of the congress international association (IAHR) journal of hydraulic research, 2004, 42, pages 516–530.
- [3] Soares, A., Covas, D., Ramos, H., Reis, L. "Unsteady flow with cavitation in viscoelastic pipes" *International journal of fluid machinery and Systems IAHR* 2009, vol. 3, pages 269–277.
- [4] Keramat, A., Tijsseling, A., Ahmadi, A. "Investigation of transient cavitating flow in viscoelastic pipes" proceeding of the 25th IAHR symposium on hydraulic machinery and system Timisoara Romania September 2010, pages 1–11.
- [5] Adamkowski, A., Lewandowski, M., "Experimental examination of unsteady friction models for transient pipe flow simulation", *Journal of fluids engineering*, 2006, vol. 128, pages 1351–1363.
- [6] Wineman, A.S., Rajagopal, K.R., *Mechanical response of polymers: an introduction*, Cambridge university press, 2000.
- [7] Covas, D., Stoianov, I., Mano, J., Ramos, H., Graham, N., Maksimovic "The dynamic effect of pipe-wall viscoelasticity in hydraulic transients. Part II—Model d, development, calibration and verification" proceedings of the congress international association (IAHR) *Journal of hydraulic research*, 2005, 43, pages 56–70.
- [8] Afshar, M.H., Rohani, M. "Water hammer simulation by implicit method of characteristic" *International journal of pressure vessels and piping*, 2008, vol. 85, pages 851–859
- [9] Ahmadi, A., Keramat, A. "Investigation of fluid–structure interaction with various types of junction coupling" *International journal of pressure vessels and piping*, 2010, vol. 85, pages 1123–1141.
- [10] Ahmadi, A., Keramat, A. "Investigation of the junction coupling due to various types of the discrete points in a piping system" *The 12th international conference of international association for computer methods and advances in geomechanics (IACMAG)1-6 GOA, India October, 2008, Pages 4016- 4024*
- [11] Bergant, A., Simpson, A. R., Vitkovsky, J. P., "Developments in unsteady pipe flow friction modelling", *Journal of hydraulic research*, 2001, vol. 39, pages 249–257.
- [12] Bergant, A., Vítkovský, J., R. Simpson, A., Lambert, M. "Valve induced transients influenced by unsteady pipe flow friction" *2director of research, water software systems, de montfortuniv, Queens building, Norway 2001, pages 1-12.*
- [13] Covas, D., Ramos, H., Betâmio de Almeida, A. "Impulse response method for solving hydraulic transient's viscoelastic pipes" proceedings of the congress international association (IAHR) for hydraulic research, 31ST, 2005, Vol 1, pages 168–169.
- [14] Covas, D., Stoianov, I., Graham, N., Maksimović, C., Ramos, H. Butler, D. "Inverse transient analysis for leak detection and

calibration – a case study in a polyethylene pipe” Proceeding of the 5th international conference on hydro informatics (IWA) cardiff wales UK. 2002, pages 1154-1159.

[15] Keramat, A. “Finite element based dynamic analysis of viscoelastic solids using the approximation of volterra integrals” Journal of fluid and structures, 2010, 26, pages 1123-1141.

[16] Ramos, H.,Borga, A. “surge effects in pressure systems for different pipe materials” Advance in water resources and hydraulic engineering 2009, pages 2172-2176

[17] Tijsseling, A.S. “Water hammer with fluid-structure interaction in thick-walled pipes”, Journal of computers &structures, 2007, pages 844-851.

[18] Tijsseling, A.S., Lambertb, M., R. Simpsonb, A., L. Stephensb, Vi'tkovsky'c, J., Bergan, A. “Skalak's extended theory of water hammer” journal of sound and vibration, 2008, vol. 310 (3), pages 718-728.

[19] Moien Barkhori, Shervin Maleki, Masoud Mirtaheri, Meissam Nazeryan, S Mahdi S Kolbadi “Investigation of shear lag effect on tension members fillet-welded connections consisting of single and double channel sections” Structural Engineering and Mechanics, 2020, vol. 1, pages 445-455.

[20] Mohammad Amin Hariri-Ardebili, S Mahdi Seyed-Kolbadi, Victor E Saouma, Jerzy W Salamon, Larry K Nuss “Anatomy of the vibration characteristics in old arch dams by random field theory” Engineering Structures, 2019, vol. 1, pages 460-475.

[21] S Mahdi S Kolbadi, Ramezan Ali Alvand, Afrasiab Mirzaei “Three Dimensional Dynamic Analysis of Water Storage Tanks Considering FSI Using FEM” International Journal of Civil and Environmental Engineering, 2018, vol. 1, pages 377-386.

[22] M Noori MA Hariri-Ardebili, SM Seyed-Kolbadi “Response surface method for material uncertainty quantification of infrastructures” Shock and Vibration, 2018, vol. 1, pages 1-30.